



Water-Land-Classification in Coastal Areas with Full Waveform Lidar Data

ALENA SCHMIDT, FRANZ ROTTENSTEINER & UWE SÖRDEL, Hannover

Keywords: lidar, classification, coast, water, conditional random fields

Summary: In this paper, we investigate full waveform lidar data acquired over the German Wadden Sea areas in the south eastern part of the North Sea. We focus especially on classification of the 3D point clouds with the aim to determine water-land-boundaries. This is a first step towards digital terrain model generation in order to analyse the terrain topography in coastal areas and, by comparing different epochs, its dynamics. For the classification of the lidar points, we learn typical class features in a training step and combine local descriptors with context information in a conditional random fields (CRF) framework, a probabilistic supervised classification approach capable of modelling contextual knowledge. We compare the results with those obtained by a fuzzy logic based approach developed specifically for the water-land-classification in Wadden Sea areas. With the latter approach we achieve a correctness rate of more than 82% for water detection. By integrating context, the results can be significantly improved by approximately 10%. Moreover, we investigate the waveform features of the data which reveals unexpected non-linear effects concerning the decomposition of the waveforms.

Zusammenfassung: *Klassifizierung der Küstenlinie in Wattgebieten mit Full-Waveform Lidar-Daten.* In diesem Paper werden Full-Waveform Lidar-Daten in Wattgebieten des südöstlichen Teils der Nordsee untersucht. Zielsetzung ist dabei die Klassifikation der 3D Punktwolke, um Land-Wasser-Grenzen abzuleiten. Dies stellt den ersten Schritt hinsichtlich der Generierung von Digitalen Geländemodellen dar. Hiermit lässt sich die Topographie der Küstenbereiche und im Vergleich unterschiedlicher Epochen deren Dynamik analysieren. Für die Klassifikation der Laserdaten wird die statistische Verteilung typischer Merkmale in einem Trainingsschritt erlernt und lokale Ausprägungen mit Kontextinformation in einem auf Conditional Random Fields beruhenden Ansatz kombiniert. Die Ergebnisse werden mit denen eines speziell für Wattgebiete entwickelten Verfahrens verglichen, welchem die Methodik der Fuzzy Logik zugrunde liegt. Während dieses Verfahren Korrektheitsraten von über 82% für Wasserflächen aufweist, kann mit unserem kontextbasierten Verfahren der Wert um etwa 10% gesteigert werden. Darüber hinaus werden Merkmale der Waveform der Signale untersucht. Hierbei lassen sich unerwartete nicht-lineare Effekte bei der Auswertung der Signalform beobachten.

1 Introduction

1.1 Motivation and Goals

In coastal areas morphological changes are caused by tidal flows, storms, climate change, and human activities. A recurrent monitoring becomes necessary in order to detect undesired changes at early stages, enabling rapid countermeasures to mitigate or minimize potential harm or hazard. The morphology of the terrain can be represented by digital terrain models (DTMs). As the terrain is very

flat, a high accuracy of the DTM is required for tasks such as hydrographic modelling. Airborne lidar (light detection and ranging) has become a standard method for DTM generation in coastal zones. The lidar technique has two main advantages compared to traditional aerial photogrammetry: Firstly, the active laser technique works independently from illumination from the sun, which allows mapping also during night-time. Secondly, the elevation model can be directly inferred from the two-way time-of-flight of the pulse reflected at the ground, whereas stereo techniques rely

on matching of corresponding points in two or more image, which requires sufficient texture. These are the reasons why we use lidar data for our application in coastal regions: the monitoring of Wadden Sea areas.

The German Wadden Sea is a unique habitat in the south eastern part of the North Sea. In 2009 it was inscribed on UNESCO's World Heritage List together with the Dutch part. Due to its biological diversity, a monitoring of the Wadden Sea becomes necessary. A corner stone of such monitoring is the detection of any changes of the terrain geometry. Gap-less DTM modelling usually requires a combination of height data gathered by bathymetry, e. g. ship-based echo sounding, in the sublittoral zone and airborne lidar systems in the eulittoral zone. However, even during low tide, residual water remains in some tidal trenches in the eulittoral zone. Because the near-infrared laser pulses used by standard lidar devices cannot penetrate water, the measured elevation represents the water surface instead of the actual terrain level underneath as would be desired. The generation of a DTM thus requires the detection of water surfaces, which leads to a classification of the lidar point cloud into *land* and *water* areas. If such a classification has been carried out, an additional data source, e. g. sonar, could be used to complete the DTM in the water areas. In the future the problem of wrong height values over water areas could be overcome to some extent by laser bathymetry. Such modern devices operate with a green laser signal that is capable to penetrate the water column (e. g. STEINBACHER et al. 2012). However, since the accessible depth underneath the water surface depends on turbidity, such technique is better suited for clearer waters compared to the Wadden Sea.

In this paper we examine two important aspects of lidar processing in coastal areas. Firstly, we investigate the classification of three-dimensional (3D) point clouds with the aim of extracting water-land-boundaries. For this purpose we implement a supervised classification method based on context: conditional random fields (CRF). We compare the results of our approach with the results obtained by the fuzzy-logic-based method developed by BRZANK et al. (2008), which was investigated especially for the classification of Wad-

den Sea areas. We also investigate the application of full waveform information for the detection of water areas and introduce the echo width as classification feature. Further characteristics derived from the full waveform such as multiple reflections are not considered because we assume to benefit not from them in mudflat areas. Secondly, we illustrate an unexpected effect concerning the signal width in our data. In nadir view, specular reflection from the water surface should cause high amplitude but minimal width of the echo. However, we frequently observe abnormally wide echoes instead. Therefore, we chose not to apply any standard calibration scheme, but to correct the range dependency only.

This paper is organised as follows. In section 2 we discuss related approaches that deal with the classification of lidar data for water detection, the labelling of point clouds by CRFs, and the correction of intensity values of the incoming signal. We describe our classification algorithm in section 3. Section 4 contains some results of our approach including a quantitative evaluation and comparison. We conclude the paper in section 5.

1.2 Dataset

Our test site is located in the south of the island of Spiekeroog in the German Wadden Sea (Fig. 1). It contains several tidal channels of various sizes. The data were acquired by a RIEGL LMS-Q560 lidar system on 19–20 February 2011 at low tide. Over the test site of 0.4 km × 1.2 km, approximately 1.7 million points were acquired with an average point density of about 3.5 points/m². The data were processed by a surveying company with the manufacturer's software. We have no direct access to the original waveform, but only to the following parameters estimated for each detected echo pulse: the 3D coordinates as well as its estimated *amplitude* and *width*. Fig. 2 shows the widths of the laser echoes of the entire flight strip of the test area. In nadir regions, the values are surprisingly high, which corresponds to a large spread of the echo *width*. This observation contradicts the common physical model that the echo *width* increases with the scan angle in flat areas of

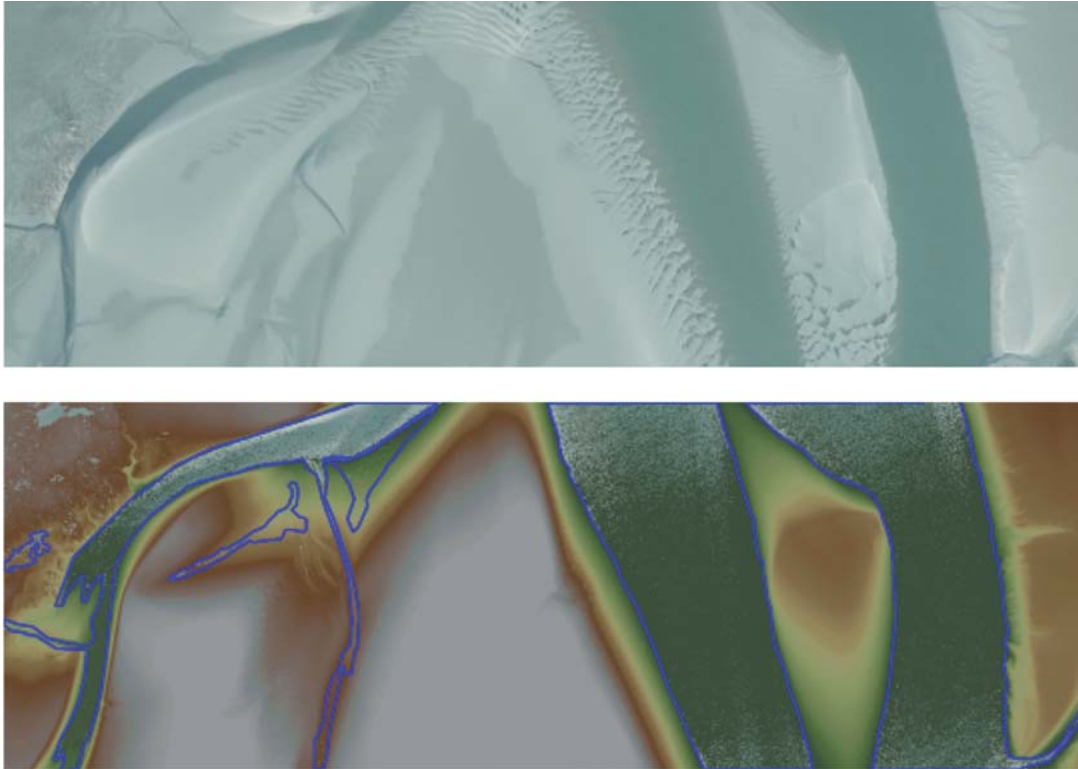


Fig. 1: Orthoimage and lidar point cloud (height span from -1.6 m (green) to 0.4 m (white)) of the test area [0.4 km \times 1.2 km] in the Wadden Sea. The areas outlined in blue are covered by water.

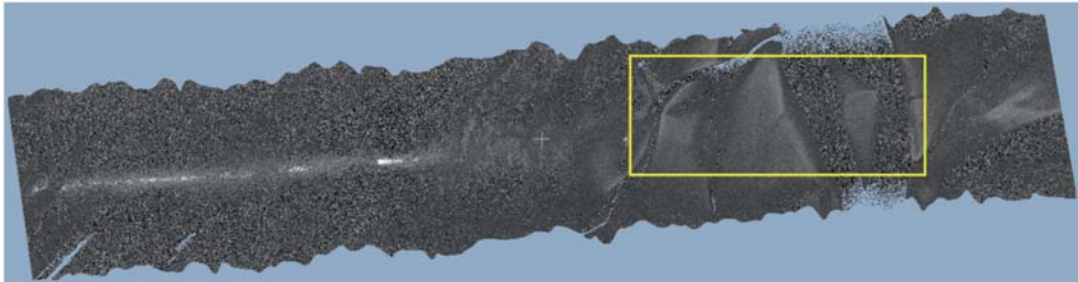


Fig. 2: Distribution of the signal width in the flight strip (increasing from dark to light). The test site for the classification is outlined in yellow.

homogenous land cover. It seems that this behaviour is connected to very large amplitude values. Therefore, we assume that signal saturation in the receive path of the sensor device might cause undesired effects. Such a non-linearity would violate the underlying assumptions of the Gaussian decomposition, i. e., saying that the echo waveform is the result of the convolution of a Gaussian pulse with a sequence of point-like reflectors modelled by their differential laser cross section.

2 Related Work

Whereas there are many approaches dealing with the classification of lidar data for the detection of objects such as buildings or vegetation, there are only a few studies on the classification of water surfaces, in particular in Wadden Sea areas. One exception is BRZANK et al. (2008), who present a point-based classification scheme as a first step towards DTM generation in the Wadden Sea. This method is

the baseline for a comparison of our CRF approach. It is a supervised classification technique based on fuzzy logic, where a membership value for the class *water* is determined for each laser point according to the features *height*, *intensity*, and *point density*. The classification into *water* and *land* is performed using a threshold for membership. All parameters of the method are derived automatically from training areas. The method takes into account the influence of height for the separation of water and land points, especially in the areas of transition. HÖFLE et al. (2009) present a segmentation-based method for the detection of water surface detection of rivers. Here, the point cloud is segmented and classified based on different features derived from the heights and the intensities of the points. Finally, the water-land-boundaries are defined by the segment borders. Classification errors occur in the case of multiple reflections, because in general they show lower intensity values for the last echo compared to the first echo, so that low signal intensity is not always caused by water surfaces. BROCKMANN & MANDLBURGER (2001) use a digital surface model (DSM) and a digital model of the water surface (DWM) for the determination of water-land-boundaries. In their method, the DWM is derived by averaging representative river heights from the laser data with regard to the known coordinates of the river axis. The water-land-boundary corresponds to the line of zero height after subtracting the DWM from the DSM. Apart from the detection of water areas, methods for the extraction of water boundaries from lidar data, e. g. river borders, have been developed. An example in the field of Wadden Sea is presented by MASON et al. (2006). They develop a method to extract tidal channel networks from lidar data. Different edge detection operators are applied to a DTM grid. This is followed by a strip detection where two edges from each side of the tidal channel are associated together. Additional high level processing improves the network, e. g. by joining the centrelines, and expanding the channels. By processing lidar data in this way, tidal channel networks are well detected in not markedly complex test areas.

To our knowledge no approach considering context in the water-land-classification pro-

cess exists. In this way, a lidar point can be assigned based on its features as well as on those obtained for all points in a defined neighbourhood. A popular context-based approach is provided by the conditional random field (CRF) framework. For image labelling the use of CRFs was introduced by KUMAR & HEBERT (2006). In comparison to image data, the labelling of point clouds is even more challenging due to the irregular distribution of points in 3D space. Several approaches for the classification of point clouds based on CRFs have been developed in the past. Some of them rely on point cloud segments. For instance, LIM & SUTER (2009) propose a method for the classification of terrestrial laser scanning data. First, they reduce the amount of data by over-segmenting the point-cloud into regions called super-voxels. Resting upon features measured by the scanner system (intensity and colour) as well as features extracted from the points inside the super-voxels, the data are labelled in a CRF framework. The potential of CRFs for airborne laser scanning data was shown by SHAPOVALOV et al. (2010). They propose a method based on segments of points and show the improvement of this non-associative approach in comparison to an associative network for an urban dataset. NIEMEYER et al. (2011) propose a point-wise method for the classification of lidar data, distinguishing three urban object classes. They also compare the performance with respect to a support vector machine, highlighting the improved classification performance of the context-based classifier.

For the labelling of lidar data, features derived from the waveform of the received pulses are of high interest for enhancing land cover classification. However, especially for the amplitude, the true physical meaning is often vague because the manufacturers seem to measure different entities. In addition, often the terms amplitude, intensity, and energy are mixed-up or used interchangeably. Nevertheless, the data should be calibrated in order to compensate for systematic effects and to achieve comparable results (WAGNER et al. 2008). The correction of the intensity eliminates the influence of sensor settings, atmosphere, and the distance to the illuminated surface (HÖFLE & PFEIFER 2007). One approach for Riegl data proposed by JUTZI &

GROSS (2010) is deriving the so-called intensity from the given amplitude and width. In addition, they consider effects depending on the range and on the atmosphere. Assuming a Lambertian reflection model, the intensity can be normalized by the incidence angle, which is the angle between beam direction and the surface normal vector. Since we observe an unexpected behaviour of the signal width in our coastal dataset, we correct the range dependency only instead of applying any standard calibration scheme.

3 Methods

In our approach for the water-land-classification the range dependency of the measured *amplitude* is corrected in a pre-processing step (section 3.1). Then, features of the classification are derived from the point cloud (section 3.2). The point cloud is classified in a supervised approach based on CRFs (section 3.3).

3.1 Pre-processing of the Data

In coastal areas two particularities of the signal must be considered during processing. Firstly, water leads to specular reflection and must not be modelled as a Lambertian surface. Thus, a correction model for the signal intensity following Lambert's cosine law is

prohibitive for water-covered areas and, as we have no a priori information about the land surface type before the classification, for the Wadden Sea areas in general. Secondly, in the course of our investigations we observed an unexpected behaviour of the involving feature *width* in our coastal dataset (section 1.2). Therefore, we decided not to apply any standard calibration scheme embedding this feature, e. g. based on JUTZI & GROSS (2010), WAGNER (2010), and LEHNER & BRIESE (2010). Instead, we use a simplified model to consider the dependence of the amplitude values from the range. Since the laser footprint is small compared to the flat terrain, no signal loss occurs in the path from sensor to object (neglecting the atmosphere). Nevertheless, on the way back only a small fraction of the backscatter is collected by the sensor. This loss can be modelled to be proportional to the squared range. Hence, we correct the amplitude a considering the range R and the distance in nadir R_n (a constant for flat areas). Since we deal here with flat terrain, this dependency can be equivalently expressed using the scan angle α :

$$a_R = a \cdot \left(\frac{R}{R_n} \right)^2 = \frac{a}{\cos^2 \alpha} \quad (1)$$

where a_R is the amplitude received over the range R .

In this way, the commonly low amplitude values for water-covered areas with high inci-

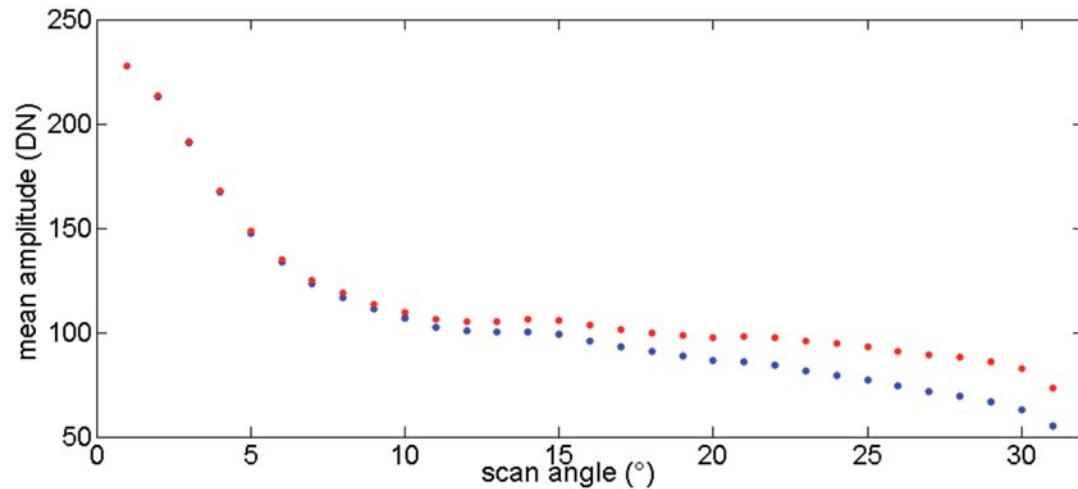


Fig. 3: Plot of mean amplitude values given in digital number (DN) over scan angle: before (blue) and after (red) the correction of the range dependency in the flight strip.

dence angles (and high difference between R and R_n) are increased. Fig. 3 shows the mean amplitude values given in digital numbers in intervals of 1° of the scan angle before and after the correction. Given the flight and sensor parameters of our dataset, these results in their maximum increase by about one third.

3.2 Feature Extraction

For the land-water-classification we use five features: *height*, *amplitude*, *point density*, *signal width*, and *variation of the width*. The first three features have been found to be well-suited for separating water from dry mud areas in the Wadden Sea (BRZANK et al. 2008). The algorithm relies on the hypothesis that water surfaces are lower than land surfaces. This assumption is suitable for water bodies at the same height level, which is usually the case in coastal areas. For laser pulses in the near-infrared, which is the part of the spectrum in which most lidar systems operate, water has a strong attenuation coefficient. This results in lower intensity values for reflections on water surface types (WOLFE & ZISSIS 1993), which can be also observed in our dataset. Fig. 4 shows the distribution of the amplitude values as a function of the scan angle. It can be seen that, firstly, the amplitude of water-covered areas is lower compared to land surfaces, and that the mean amplitude decreases with increasing scan angles, as discussed in

section 3.1. However, the high portion of specular reflection on calm water surfaces is another characteristic already discussed above. Thus, relatively high intensity values can be observed for points near the nadir direction (HÖFLE et al. 2009). The point density is defined as the number of backscattered signals per area. We define a vertical cylinder with the radius r to find adjacent points which are then used to calculate local features. Several radii were tested; however, the impact of r on the resulting features was marginal. We finally set $r = 3$ m. Especially on water surfaces, specular reflections dependent on the incidence angle can cause a significant decrease of the *point density*. The additional full waveform features which influence the investigated detection of the water-land-boundaries include the *signal width* and its *variation* with a standard deviation in a local 2D neighbourhood of lower than $r = 3$ m.

3.3 Classification by Conditional Random Fields

CRFs are a flexible technique for the classification of any kind of 2D or 3D spatial data. Thereby, a class label C_i from a given set of classes \mathbb{C} is assigned to each data site, i. e. pixel or point $i \in [1, \dots, n]$. In our case the sites are the lidar points, which are classified by finding the optimal label configuration that maximises the posterior probability $P(\mathbb{C}|\mathbf{x})$ of

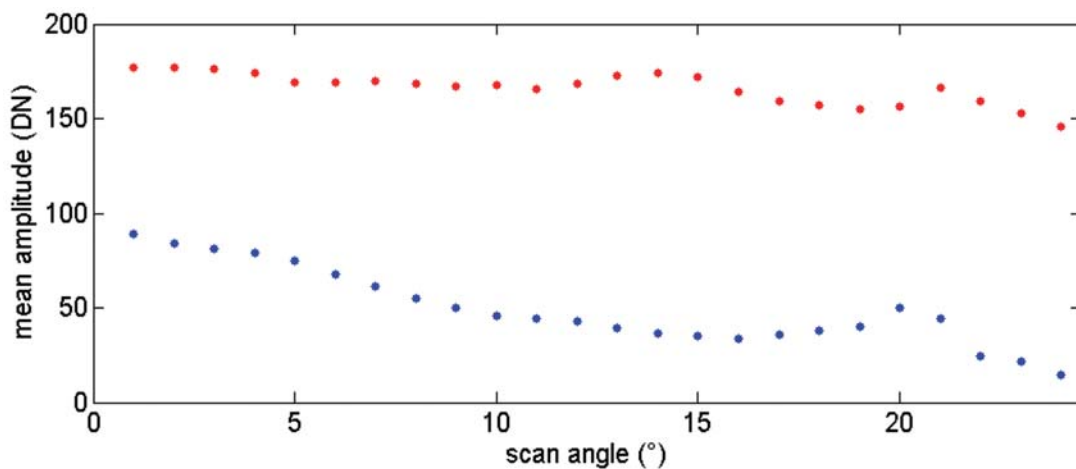


Fig. 4: Average of amplitude values given in digital number (DN) for water (blue) and land (red) surfaces in the test area as a function of the scan angle.

the point labels $\mathbf{C} = [C_1, C_2, \dots, C_n]$ given the observed data $\mathbf{x} = [x_1, x_2, \dots, x_n]$. CRFs belong to the group of graphical models whose nodes correspond to the points and whose edges model the dependencies between labels and/or data of adjacent points. The posterior probability can be modelled by

$$P(\mathbf{C} | \mathbf{x}) = \frac{1}{Z} \exp(E(\mathbf{x}, \mathbf{C})), \quad (2)$$

where $E(\mathbf{x}, \mathbf{C})$ is an energy term and Z is a normalising constant. The energy term can be expressed as the sum of *association potentials* $A(\mathbf{x}, C_i)$ and *interaction potentials* $I(\mathbf{x}, C_i, C_j)$ over the neighbourhood N_i and the dataset S :

$$E(\mathbf{x}, \mathbf{C}) = \sum_{i \in S} A(\mathbf{x}, C_i) + \sum_{i \in S} \sum_{j \in N_i} I(\mathbf{x}, C_i, C_j). \quad (3)$$

The *association potential* $A(\mathbf{x}, C_i)$ indicates the likelihood of a point i belonging to a class C_i given the observations \mathbf{x} . The *interaction potential* $I(\mathbf{x}, C_i, C_j)$ measures how the classes of neighbouring points and data interact. The structure of the graph, the observed features, and the potentials have to be defined for the application.

In our approach, we have the peculiarity of an irregular data structure in the raw laser scanning point cloud. Here, each point is linked to its k nearest neighbours in 2D. A fast access to the nearest neighbours of each lidar point is obtained by indexing the point cloud using a k -d tree. Although we apply 3D data, the reduction to a 2D search is justified by the appearance of the data. In the Wadden Sea there are hardly any objects with a significant extension in height.

A feature vector $\mathbf{h}_i(\mathbf{x})$ which contains the features described in section 3.1 is assigned to each node i . In order to consider context, interaction features modelling the relationship of nodes are introduced for each edge linking the node i and j . Here, we calculated the interaction feature vector $\boldsymbol{\mu}_{ij}(\mathbf{x})$ as the difference of feature vectors of neighbouring nodes i and j

$$\boldsymbol{\mu}_{ij}(\mathbf{x}) = \mathbf{h}_i(\mathbf{x}) - \mathbf{h}_j(\mathbf{x}). \quad (4)$$

The node features $\mathbf{h}_i(\mathbf{x})$ of the class label C_i at site i are linked by the *association potential*

$A(\mathbf{x}, C_i)$. In general, any local discriminative classifier resulting in a probability $P(C_i | \mathbf{h}_i(\mathbf{x}))$ can be used to define the association potential via $A(\mathbf{x}, C_i) = \log P(C_i | \mathbf{h}_i(\mathbf{x}))$. Closely related to KUMAR & HEBERT (2006) we use a generalized linear model for that purpose. Then, $A(\mathbf{x}, C_i)$ can be expressed as

$$A(\mathbf{x}, C_i = l) = \mathbf{w}_l^T \mathbf{h}_i(\mathbf{x}). \quad (5)$$

In (5) vector \mathbf{w}_l contains the weights of node features and is determined by a training step. Such a vector is defined for each class l . The probability that a pair of adjacent nodes i and j has the labels C_i and C_j is described by the *interaction potential* $I(\mathbf{x}, C_i, C_j)$. Analogous to the *association potential* $A(\mathbf{x}, C_i)$ it can be modelled being proportional to $\log P(C_i, C_j | \boldsymbol{\mu}_{ij}(\mathbf{x}))$, obtained again by a generalized linear model:

$$I(\mathbf{x}, C_i = l, C_j = k) = \mathbf{v}_{l,k}^T \boldsymbol{\mu}_{ij}(\mathbf{x}), \quad (6)$$

where $\mathbf{v}_{l,k}$ is the weight vector of the interaction features. Such a vector $\mathbf{v}_{l,k}$ exists for each combination of classes (l, k) .

In the training process the optimal values for the weight vectors are derived from training data. The use of exact probabilistic methods for this is computationally intractable. Thus, they are replaced by approximate solutions. Here, we applied the gradient descent optimisation method of L-BFGS (limited memory Broyden-Fletcher-Goldfarb-Shanno) (LIU & NOCEDAL 1989) for the minimisation of the objective function $f = -\log [P(\theta | \mathbf{x}, \mathbf{C})]$, where θ contains the weight vectors \mathbf{w}_l and $\mathbf{v}_{l,k}$.

The optimal label configuration is determined in an inference step. Thereby, $P(\mathbf{C} | \mathbf{x})$ is maximised for given parameters based on loopy belief propagation (FREY & MACKAY 1998), a standard iterative message passing algorithm for graphs with cycles. The result is one probability value per class for each data point.

4 Experiments

For the evaluation of our approach we use the dataset described in section 1.2. Because lidar data of the Wadden Sea are not readily acces-

sible, we are limited to consider only one dataset. Ground truth is generated by labelling the point cloud manually. As a minimum requirement the connected network of tidal channels have to be found, for example, to fuse the DTM at these areas with bathymetric data. However, isolated local water regions which are often higher than the large tidal channels remain. Of course, the quality of the laser DTM is questionable in such areas, too.

Both methods are supervised approaches and thus require a training step. For training we took about 2% of the points from the entire dataset. Then, the computational costs in the CRF approach depending on the number of features (here: 3–5) and the size of neighbourhood (here: 2) vary between 0.6 and 3.8 minutes. For the algorithm of BRZANK et al. (2008), the computational costs are approximately 0.3 minutes. We processed the tests on a machine with a 2.8 GHz Quad-Core CPU and 8 GB RAM.

In section 4.1 we compare the results of our algorithm with those obtained by the method of BRZANK et al. (2008), wherefore the original software was available for us. In this way, we analyze the influence of contextual information for the land-water-classification. Moreover, we assess the impact of full waveform information on the CRF classification (section 4.2), in particular of the width. For the qualitative evaluation we use the *completeness* and *correctness* rates as well as the *quality* (HEIPKE et al. 1997).

4.1 Comparison of both Approaches

We classify the data using the fuzzy-logic-based method of BRZANK et al. (2008) and our CRF framework. Here, we use the same features (group I: *height, amplitude, point*

density) and training data. Tab. 1 and Fig. 5 show the classification results. It can be seen that both classes have a high rate of correctness and completeness of more than 80% and in most cases of more than 90% in both approaches. By integrating context of the CRF framework the classification rate of *water* rises by approximately 10%. Especially the classification results in the transition zone can be significantly improved. Due to the feature *height*, for which a high weight is derived in the training step of the fuzzy-based approach, misclassifications occur in areas with low local height differences. Thus, the borders of the tidal channels are shifted further onto the land. Moreover, isolated small water areas in different height levels are not detected using the method of BRZANK et al. (2008). These problems can be overcome by integrating contextual knowledge using the CRF approach.

4.2 Comparison of Different Classification Features

We investigate the influence of waveform information on the water detection with our CRF approach in a second test. Here, we use only information about the waveform (group II: *amplitude, width, and variation of width*) as classification features. Fig. 6 illustrates that the variation of the signal width indicates water areas. By a classification using this features group also a high rate of completeness and correctness of more than 85% can be obtained for both classes (Tab. 1). The correctness of *water* decreases due to misclassification of some points with low intensity and high variation of their signal width (both characteristically for water areas) on some land areas. However, the correctness of *land* as well as the completeness of *water* can be improved. Over-

Tab. 1: Correctness (CR), completeness (CP) and quality (Q) for land (L) and water (W) in the fuzzy logic and the conditional random fields (CRF) framework using different feature combination (I = *height, amplitude, point density*, II = *amplitude, signal width, variation of width*).

	Fuzzy Logic (I)			CRF (I)			CRF (II)			CRF (I + II)		
	CR	CP	Q	CR	CP	Q	CR	CP	Q	CR	CP	Q
L	98.3	94.6	93.1	98.8	97.9	96.7	99.3	94.7	94.1	99.2	97.2	96.4
W	84.3	94.7	80.5	93.5	96.2	90.2	85.2	97.9	83.7	91.5	97.4	89.3

all, it can be seen that even by neglecting geometrical information and the important feature *height* the water-land-classification delivers good results which we could not observe in our previous work in urban areas (SCHMIDT et al. 2011). Combining both features groups, the

correctness and completeness rates are comparable to the good results of the classification with the features *height*, *amplitude* and *point density*. Moreover, the correctness of *land* and the completeness of *water* can be improved by the full waveform features.

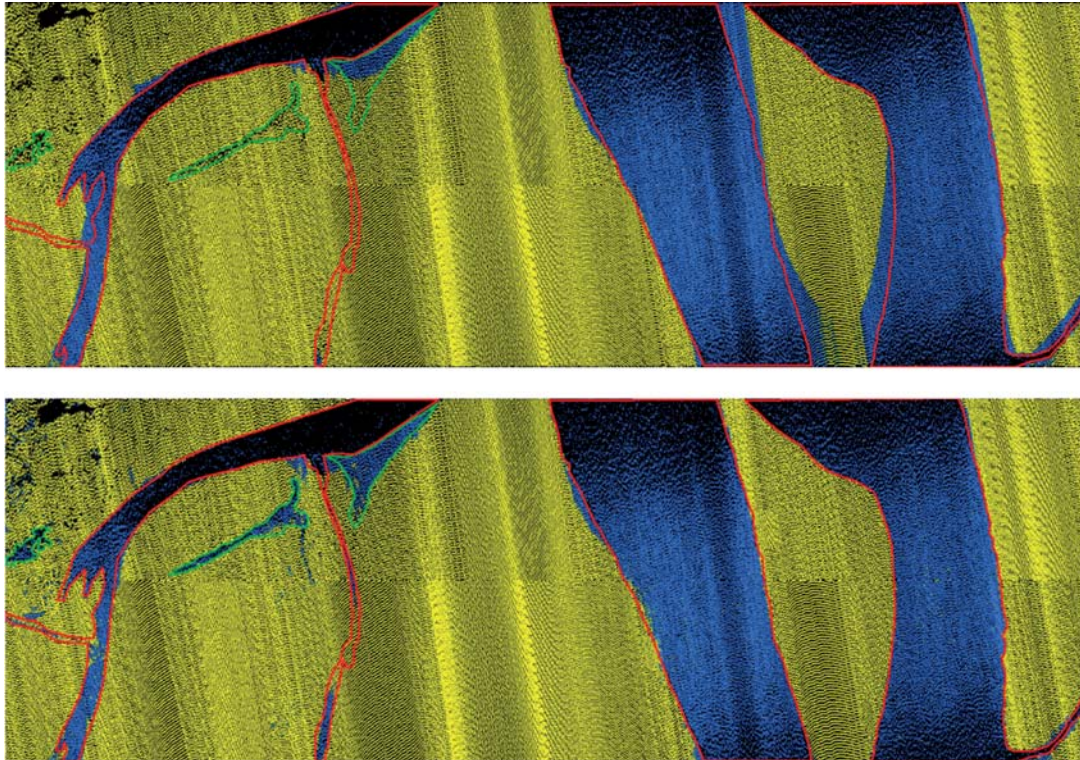


Fig. 5: Classification results of the test area [0.4 km × 1.2 km] for *water* (blue) and *land* (yellow) using the fuzzy logic (top) and the CRF framework (bottom) with feature group I. Big tidal channels (outlined in red) are well detected by both approaches. Some small water covered areas on a higher height level (outlined in green) are only labelled as *water* by the CRF method.

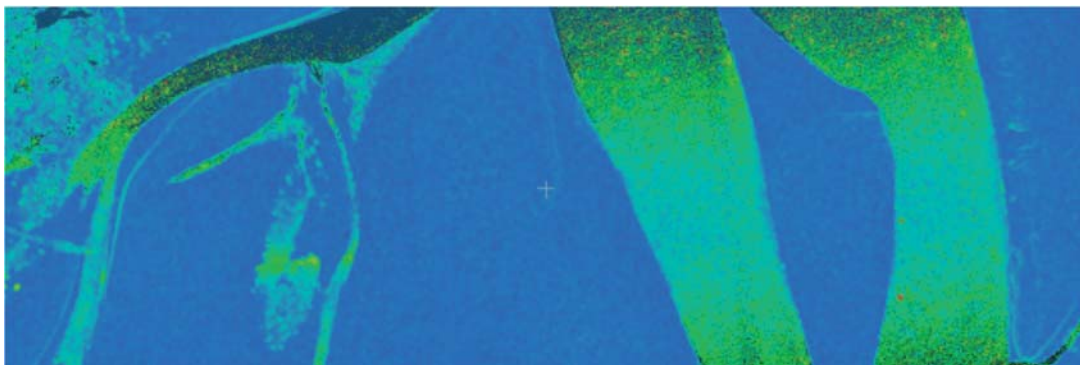


Fig. 6: Distribution of the feature *variation of signal width* coloured from low (blue) to high (green).

5 Conclusion

In this paper we are proposing a method for the water-land-classification of full waveform lidar data in coastal areas. For this task we presented suitable classification features and learnt typical structures of the data in a training step. We integrated contextual knowledge in a supervised classification process based on CRF. As result of the classification process, each point is assigned to one of the two classes *water* and *land*. We compared the results to a non-contextual method and showed that small water bodies on different height levels can be detected by our approach, whereas the algorithm based on the assumption of equal height levels fails. In this way the correctness rate of water can be significantly improved. Moreover, we investigate the full waveform information on water areas. It can be seen that only by using full waveform features (amplitude, signal width and its variation) good results can be obtained. Concerning the width of the signal, we observed an unexpected behaviour in our dataset where high values of the width occur in nadir regions. We assume undesired effects in the receive path of the sensor due to signal saturation.

In the future we intend to further examine this non-linearity because such an effect may occur also for other types of land cover. Moreover, we want to extend the classification to additional land surface types, e. g. by integrating texture features to get detailed information about the structure of the coastal surfaces.

References

- BROCKMANN, H. & MANDLBURGER, G., 2001: Aufbau eines digitalen Geländemodells vom Wasserlauf der Grenzoder. – Tagungsbericht zur 21. Wissenschaftlich-Technischen Jahrestagung der Deutschen Gesellschaft für Photogrammetrie und Fernerkundung: 199–208, Konstanz.
- BRZANK, A., HEIPKE, C., GOEPFERT, J. & SÖRGEL, U., 2008: Aspects of generating precise digital terrain models in the Wadden Sea from lidar – water classification and structure line extraction. – ISPRS Journal of Photogrammetry and Remote Sensing **63** (5): 510–528.
- FREY, B. & MACKAY, D.J.C., 1998: A revolution: Belief propagation in graphs with cycles. – Advances in Neural Information Processing Systems **10**: 479–485.
- HEIPKE, C., MAYER, H., WIEDEMANN, C. & JAMET, O., 1997: Evaluation of automatic road extraction. – International Archives of Photogrammetry and Remote Sensing **32** (3–4, W2): 151–160.
- HÖFLE, B. & PFEIFER, N., 2007: Correction of laser scanning intensity data: data and model-driven approaches. – ISPRS Journal of Photogrammetry and Remote Sensing **62** (6): 415–433.
- HÖFLE, B., VETTER, M., PFEIFER, N., MANDLBURGER, G. & STÖTTER, J., 2009: Water surface mapping from airborne laser scanning using signal intensity and elevation data. – Earth Surface Processes and Landforms **34** (12): 1635–1649.
- JUTZI, B. & GROSS, H., 2010: Investigations on surface reflection models for intensity normalization in airborne laser scanning (ALS) data. – Photogrammetric engineering & remote sensing **76**: 1051–1060.
- KUMAR, S. & HEBERT, M., 2006: Discriminative Random Fields. – International Journal of Computer Vision **68** (2): 179–201.
- LEHNER, H. & BRIESE, C., 2010: Radiometric calibration of Full-Waveform Airborne Laser Scanning Data based on natural surfaces. – 100 Years ISPRS Advancing Remote Sensing Science **38** (7B): 360–365.
- LIM, E.H. & SUTER, D., 2009: 3d Terrestrial Lidar Classifications with Super-Voxels and Multi-Scale Conditional Random Fields. – Computer-Aided Design **41** (10): 701–710.
- LIU, D.C. & NOCEDAL, J., 1989: On the Limited Memory BFGS method for large scale optimization. – Mathematical Programming **45**: 503–528.
- MASON, D.C., SCOTT, T.R. & WANG, H., 2006: Extraction of tidal channel networks from airborne scanning laser altimetry. – ISPRS Journal of Photogrammetry and Remote Sensing **61** (2): 67–83.
- NIEMEYER, J., WEGNER, J., MALLET, C., ROTTENSTEINER, F. & SÖRGEL, U., 2011: Conditional random fields for urban scene classification with full waveform lidar data. – Photogrammetric Image Analysis (PIA), Lecture Notes in Computer Science **6952**: 233–244, Springer, Berlin / Heidelberg.
- SCHMIDT, A., ROTTENSTEINER, F. & SÖRGEL, U., 2011: Detection of Water Surfaces in Full-Waveform Laser Scanning Data. – International Archives of the Photogrammetry, Remote Sensing and Spatial Information Sciences **38** (4, W19), Hannover.
- SHAPOVALOV, R., VELIZHEV, A. & BARINOVA, O., 2010: Non-associative Markov Networks for 3d Point Cloud Classification. – International Ar-

- chives of the Photogrammetry, Remote Sensing and Spatial Information Sciences **38** (3A): 103–108.
- STEINBACHER, F., PFENNIGBAUER, M., AUFLEGER, M. & ULLRICH, A., 2012: High resolution airborne shallow water mapping. – *International Archives of the Photogrammetry, Remote Sensing and Spatial Information Sciences* **39** (B1): 55–60.
- WAGNER, W., HYYPPÄ, J., ULLRICH, A., LEHNER, H., BRIESE, C. & KAASALAINEN, S., 2008: Radiometric calibration of full-waveform small-footprint airborne laser scanners. – *International Archives of Photogrammetry, Remote Sensing and Spatial Information Sciences* **37** (B1): 163–168.
- WAGNER, W., 2010: Radiometric calibration of small-footprint airborne laser scanner measurements: Basic physical concepts. – *ISPRS Journal of Photogrammetry and Remote Sensing* **65** (10): 505–513.
- WOLFE, W. & ZISSIS, G.J., 1993: *The infrared handbook*. – 1700 p., The Infrared Information Analysis Center, Environmental Research Institute of Michigan, Detroit, USA.

Address of the Authors:

M.Sc. ALENA SCHMIDT, PD Dr.-Ing. FRANZ ROTTENSTEINER, Prof. Dr.-Ing. UWE SÖRGEL, Leibniz Universität Hannover, Institut für Photogrammetrie und GeoInformation, Nienburger Str. 1, D-30167 Hannover, Tel.: +49-511-762-2482, Fax: +49-511-762-2483, e-mail: {alena.schmidt}{rottensteiner}{soergel}@ipi.uni-hannover.de

Manuskript eingereicht: November 2012
Angenommen: Januar 2013